

# Fabrication of Flowerlike Polymer Superstructures Using Polymer/Zeolite Composites Prepared with Supercritical CO<sub>2</sub>

Yong Wang, Zhimin Liu,\* Buxing Han, Junchun Li, Haixiang Gao, Jiaqiu Wang, and Jianling Zhang

Center for Molecular Science, Institute of Chemistry, Chinese Academy of Sciences, Beijing, 100080, China

Received: August 19, 2004; In Final Form: December 1, 2004

We report a route to the fabrication of unique flowerlike polymer superstructures with uniform petals at the nanoscale. In this method, polymer/zeolite composite is first prepared by loading corresponding monomer and initiator into the channels of the host zeolite with the aid of supercritical (SC) CO<sub>2</sub>, followed by thermal polymerization of monomers in the channels of the zeolite. The resultant polymer/zeolite composite is then treated with HF aqueous solution to allow the self-aggregation of the polymer and the inorganic components to form the polymeric layers and inorganic layers. Unique microscale flowerlike polymer superstructures are obtained after further treatment with HF aqueous solution. Different techniques, such as scanning electron microscopy (SEM), X-ray diffraction (XRD), transmission electron microscopy (TEM), Fourier transform infrared spectroscopy (FTIR), and thermogravimetry (TG), have been used to characterize the microflowers.

## Introduction

In recent years, there are increasing interests in the fabrication of functional composites through inclusion guest molecules in host porous frameworks with the expectation of new materials combining the desired properties both of the host and of the guest materials. In some cases, the guest molecules (the precursors) confined in the host are further chemically or physically converted to target materials with expected properties. For example, conducting filaments of polyaniline have been prepared in the 3-nm-wide hexagonal channel system of the aluminosilicate MCM-41, and it was found that the filaments have significant conductivity while encapsulated in the channels, demonstrating its possibility in the application of nanometer electronic devices.<sup>1</sup> In addition, the composites sometimes are further dissolved or calcinated to remove the host materials and to liberate the structured materials consisting of guest substances. Nanostructured materials including metals,<sup>2–5</sup> semiconductors,<sup>6–8</sup> polymers,<sup>9–11</sup> carbons,<sup>12,13</sup> and other functional materials<sup>14</sup> have been fabricated through this technique.

In the synthesis of such composites, the hosts, usually porous materials with high surface area, such as microporous zeolites and mesoporous molecular sieves, are usually used to confine or direct the growth of the guest molecules.<sup>1–14</sup> Because the size of the voids of host materials often falls into nanometer scale or even smaller, it is difficult to get a uniform distribution of guest molecules into the porosity of the host. Therefore, it is essential to choose a proper way to include guest molecules into the host to get a high-loading and uniform distribution of guest molecules in the host. Conventionally, the guests are introduced into the voids of the host through ion exchange, capillary force, or gas condensation, etc., among which the wet solution route and the chemical vapor infiltration are the most frequently used.<sup>1–3,7,8,10,12–14</sup> In the wet solution route, host materials are immersed in the solution of precursors or in liquid precursors directly,<sup>3,7,8,13,14</sup> while in the latter route, hosts are

exposed to the precursor vapor.<sup>1,2,10,12</sup> However, both methods may suffer from incomplete filling of the host voids.

As an alternative, a supercritical fluid (SCF) inclusion technique has been developed recently, which can provide high filling percentage. For example, VPI-5 microporous zeolite had been used to adsorb organic compounds from SC CO<sub>2</sub>.<sup>15</sup> In addition, it was reported that almost complete (95%) filling of the mesoporous silica powders with silicon and germanium nanowires was achieved using the supercritical (SC) hexane phase inclusion technique.<sup>16–18</sup> It was also demonstrated that the SC CO<sub>2</sub> inclusion technique could form ordered arrays of nanowires and nanotubes of cobalt, copper, and iron oxide within mesoporous silica matrixes.<sup>19</sup> The SCF phase inclusion technique is based on the fact that SCF has low viscosity, high diffusivity, near zero surface tension, and good solubility for many small organic molecules, which gives it the ability to carry small molecules into any fine spaces rapidly provided the spaces can contain them.<sup>20</sup> Especially, SC CO<sub>2</sub> is an ideal solvent for the inclusion process as it is nontoxic, nonreactive, and relatively inexpensive. On the basis of this principle, SC CO<sub>2</sub> has been utilized to impregnate different additives into polymer matrix or porous materials.<sup>21–24</sup> It has also been used to fabricate polymer–polymer composites.<sup>25–28</sup>

In this work, we developed a method to fabricate unique flowerlike polymer superstructures using the microporous zeolites as the host. In this route, we used SC CO<sub>2</sub> to impregnate vinyl monomer into the micropores of zeolite with high filling, resulting in polymer/zeolite composites after polymerization of the monomers in the zeolite. By etching the polymer/zeolite composites with HF aqueous solution, unique microflowers with polymer petals of nanoscale were obtained.

## Experimental Section

**Materials.** All of the reagents were purchased from Beijing Chemical Plants unless stated in particular. Styrene and methyl methacrylate (MMA) were distilled under vacuum prior to use. Divinyl styrene (DVB) was bought from Tokyo Kasei Kogyo

\* Corresponding author. Tel.: 86-10-62562821. Fax: 86-10-62562821. E-mail: liuzm@iccas.ac.cn.

Co. Ltd. and used without further purification. 2,2'-Azobis(isobutyronitrile) (AIBN) was recrystallized from methanol. Zeolite beads was obtained from Bayer AG German (Zeolith T146), which was Na A type and about 20%  $\text{Ca}^{2+}$  exchanged and presented as beads with a diameter of about 2–4 mm. Carbon dioxide was obtained from the Beijing Analytical Instrument Factory with a purity of 99.95% and was used as received.

**Preparation of the Microflowers.** We only discuss the procedures to prepare and characterize the PS microflowers in detail. In a typical experiment, styrene (1.5 g) and initiator AIBN (7.5 mg) were charged into a 22 mL stainless steel autoclave. Zeolite beads (0.7 g) were placed onto a stainless steel supporter fixed in the autoclave to prevent the zeolite from direct contacting with the liquid styrene. The autoclave was then put into a water bath of 40.0 °C. The air in the autoclave was replaced with  $\text{CO}_2$ , and more  $\text{CO}_2$  was charged up to 11.0 MPa. The system was maintained at these conditions for 6 h. The autoclave was then transferred into an oven of 80 °C to polymerize the encapsulated monomer for 12 h to obtain the polymer/zeolite composite. The composite has a weight increase of about 20% due to the impregnation of the polymer and adsorption of the unreacted monomer. The composite was then treated with 40% HF aqueous solution at 18 °C for the desired time.

**Characterization.** All of the SEM images in this work were obtained from a Hitachi-S4300 electron microscope operated at 15.0 keV equipped with an EDX analysis system (Oxford instruments). Samples were sprayed with a thin layer of gold before observation. For the TEM observation, samples were first dispersed in ethanol with ultrasonification for about 30 s, and dropped on a copper grid and then examined under a Hitachi 600 electron microscope operated at 100 keV. XRD patterns were obtained from a Japan D/MAX.RB diffractometer with  $\text{Cu K}\alpha$  radiation ( $\lambda = 0.154$  nm) at a generator voltage of 40 kV and a generator current of 100 mA. The scanning speed and the step were  $2^\circ/\text{min}$  and  $0.02^\circ$ , respectively. FTIR spectra were recorded by means of a Bruker Tensor 27 (32 scans,  $4\text{ cm}^{-1}$ ) FTIR spectrometer. TG measurements were performed with the thermal analyzer (NETZSCH STA 409 PC/PG) in air atmosphere with a heating rate of  $10\text{ }^\circ\text{C}/\text{min}$ . The  $\text{N}_2$  adsorption measurements were performed on an ASAP 2405N adsorption analyzer.

## Results and Discussion

**Morphology of the Materials.** In the present work, the polymer/zeolite composite was first prepared by loading corresponding monomer (e.g., styrene) and initiator into the channels of the zeolite with the aid of SC  $\text{CO}_2$ , followed by thermal polymerization. The polymer/zeolite composites were then treated with HF aqueous solution to remove the zeolite. From the conventional point of view in the synthesis of nanostructures using zeolites as the hosts, polymer nanowires or tubes, or reverse 3D networks should be expected. However, surprisingly and interestingly, flowerlike structures in microscale were formed. Figure 1 illustrates the SEM images of PS microflowers obtained with a HF treatment time of 36 h.

From Figure 1a and b, we can see that the flowers are uniform in diameter and have a narrow size distribution of about 6–8  $\mu\text{m}$ . Every individual flower possesses many radically out-extending thin petals with a thickness of about 30–60 nm, as shown in Figure 1c and d. In addition, the petals are curved in shape, indicating their flexibility. Except for some adhering contaminants, the surface is relatively smooth.

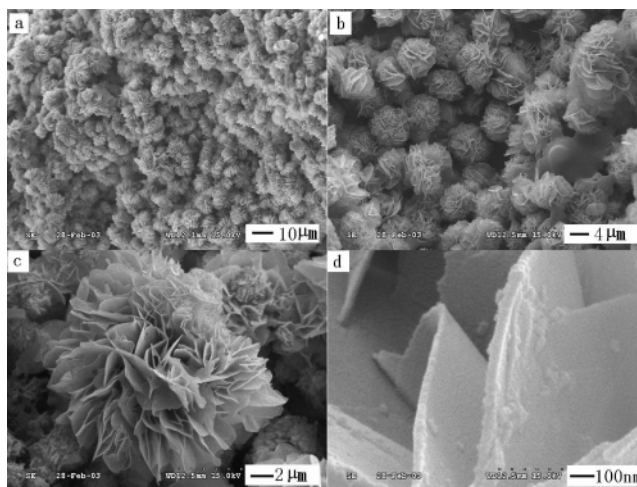


**Figure 1.** SEM images of PS microflowers at different magnifications.

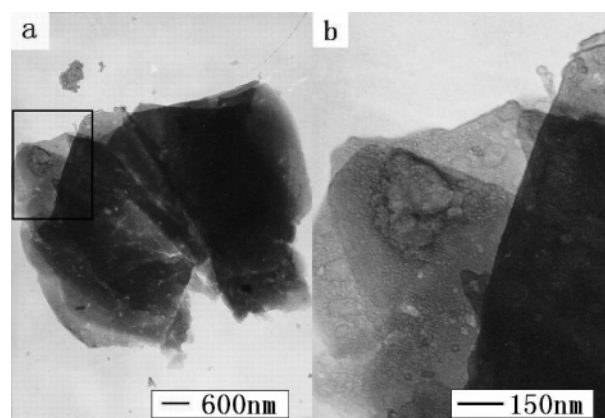


**Figure 2.** TEM images of an individual microflower. The boxed area in (a) is magnified in (b).

We also examined the resulted flowerlike structures under TEM, and the TEM images are given in Figure 2. Obviously, they are indeed composed of thin flakes (petals), which are attached together in the center. Furthermore, we can see from the TEM images that there are some particles dispersed in the petals, which suggests that the petals are not composed of pure polymer.

The obtained microflowers are obviously not the reflection of the channels of the zeolite because there is no such flowerlike pore structure in the zeolite, which will be discussed in the following sections. The formation of the microflower must be formed in the HF treatment of the composites; that is, the HF etch process plays an important role in the synthesis of such unique flowerlike structures. Therefore, it is necessary to investigate the HF etch procedure in detail.

**Characterization by XRD, FTIR, TG Analysis, and  $\text{N}_2$  Adsorption.** We treated the PS/zeolite composite with HF aqueous solution and took out some sample from the solution at intervals. These samples were washed with copious amounts of water, dried, and then analyzed with different techniques.

Figure 3 gives the XRD patterns of the original zeolite, PS/zeolite composite, and composites etched with HF solution for different times. Evidently, the original zeolite and the polymer/zeolite composite have almost identical XRD patterns except for the change of the relative intensity of some Bragg reflections, which strongly suggests the presence of polymer in the channels of the zeolite pores.<sup>29</sup> Obviously, the HF etch drastically changes the structure of the composite. The original crystalline structure of the zeolite is severely destroyed by 5 h of HF etch, reflected

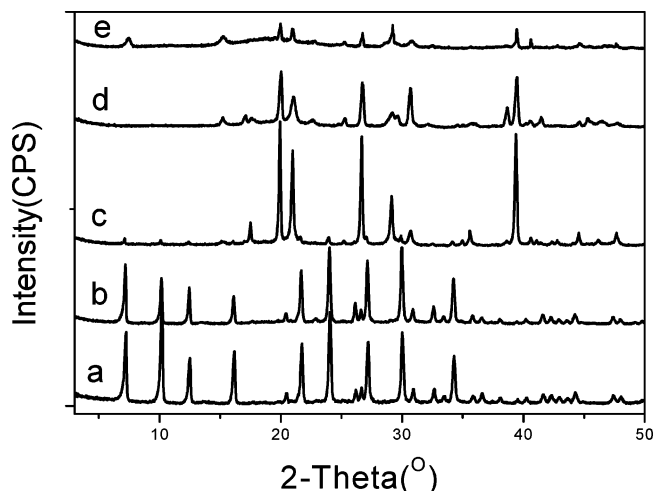


**Figure 3.** XRD patterns of original zeolite (a), PS/zeolite composite (b), and composites etched with HF for 5 h (c), 36 h (d), and 120 h (e).

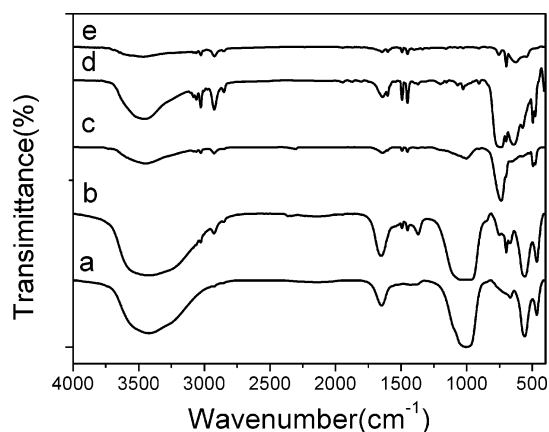


**Figure 4.** FTIR spectra of original zeolite (a), PS/zeolite composite (b), and composites treated with HF for 5 h (c), 36 h (d), and 120 h (e).

by the tremendous intensity drop of the diffraction peaks. However, with the disappearance of the original zeolite structure, a new crystalline structure is formed simultaneously, suggested by the presence of new peaks in the XRD pattern of the composite after 5 h of etch. With a HF etch time of 36 h, the original zeolite structure is completely destroyed. In the present work, in-situ energy-dispersive X-ray (EDX) analysis during the SEM observation showed that those newly formed crystals contain large amounts of F, Na, and Si, and their XRD peaks can be indexed as  $\text{Na}_2\text{SiF}_6$  crystal (JCPDS Card: 33-1280). However, the new crystal also diminished gradually under the attack of HF, as shown by the drop of the intensity of the diffraction peaks of  $\text{Na}_2\text{SiF}_6$  as the HF etching time proceeds.

FTIR spectra also reflect structure changes of the zeolite with different HF etch times, as shown in Figure 4. Zeolite characteristic peaks can be clearly seen in the spectra of the original zeolite and the PS/zeolite composite at 1005, 668, 557, and 466  $\text{cm}^{-1}$ ,<sup>30</sup> while after 5 h of HF etch, the intensity of the peaks drops significantly. Extending the etch time, the intensity becomes lower. At the same time, new peaks around 735 and 495  $\text{cm}^{-1}$  appear, which are attributed to the newly developed  $\text{Na}_2\text{SiF}_6$  crystals.<sup>31</sup>

TG analysis of various samples was carried out in air atmosphere up to 900 °C, and the results are given in Figure 5. Clearly, the weight loss below 300 °C in the samples is due to the desorption of small molecules including water, and the

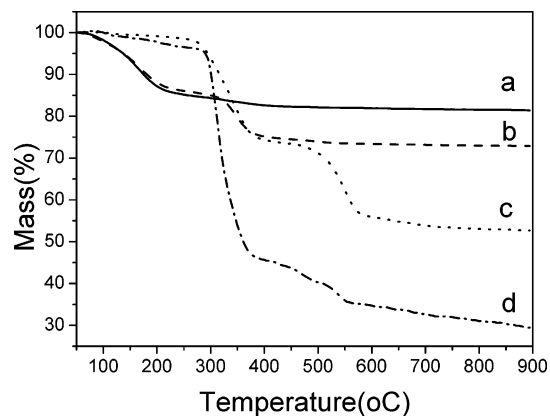


**Figure 5.** TG curves of original zeolite (a), PS/zeolite composite (b), and composite treated with HF for 36 h (c) and 120 h (d).

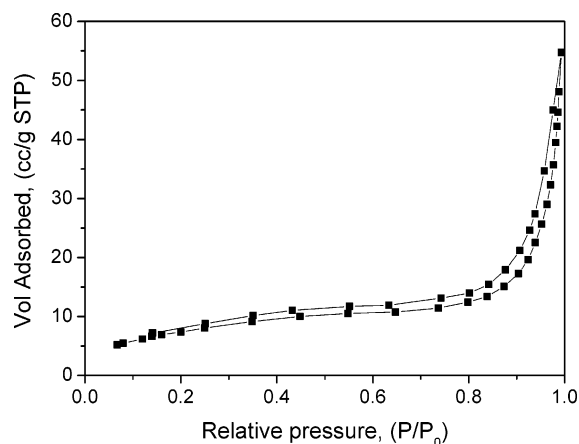


**Figure 6.** Nitrogen sorption isotherm for the microflowers obtained with an etch time of 36 h.

weight loss between 300 and 390 °C on curves b, c, and d is attributed to the combustion of the PS component. In addition, there is another weight loss above 450 °C for the two HF etched samples, resulting from the decomposition of  $\text{Na}_2\text{SiF}_6$  which releases  $\text{SiF}_4$  gas. Evidently, the weight percent of PS in the samples increases with increasing etching time, indicating the continuous dissolution of the inorganic component and the formation of the microflowers. However, there is still inorganic component in the sample even after an etching time of 120 h, which is consistent with the result of XRD analysis. This is understandable because it takes long time for the inorganic components in the inner part to be dissolved. Therefore, we can deduce that the petals of the microflower are composed mainly of the insoluble polymer, while the center part is the inorganic/polymer core. The size of the core depends on the etch time.

The  $\text{N}_2$  adsorption measurements were performed for the microflowers obtained with an etch time of 36 h (see Figure 6). The specific surface area determined was about 20  $\text{m}^2/\text{g}$ . The relative low BET surface area further supports the argument that, as discussed above, there was an inorganic/polymer core in the center part of a microflower.

**Morphology Evolution of the Polymer/Zeolite Composite in the HF Etch Process.** To understand the mechanism for the formation of the “microflowers”, it is necessary to know what happened in the HF etching procedure. We examined the morphology of the polymer/zeolite composite treated with HF for different time under SEM. The original zeolite and the polymer/zeolite composite are microparticles, as shown in Figure 7a and b. After an HF etch time of 5 h, many new crystals with

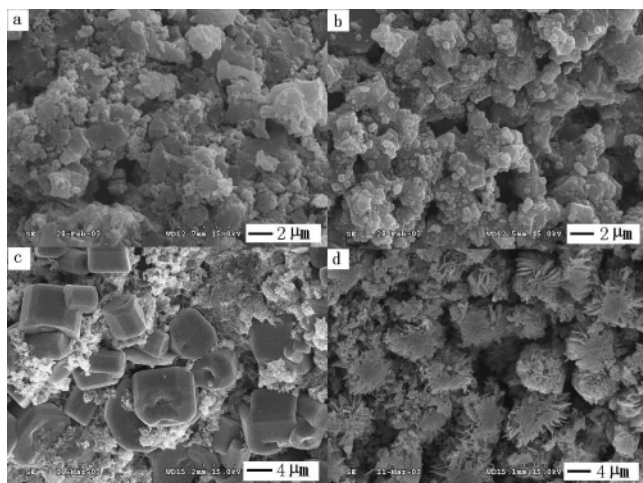


**Figure 7.** SEM images at different stages of the preparation of microflowers. (a) The original zeolite, (b) the PS/zeolite composite, and composites treated with HF solution for 5 h (c) and 24 h (d).

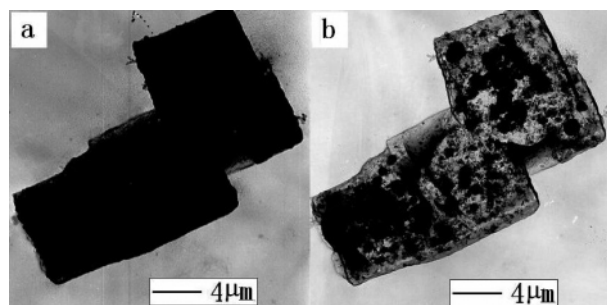


**Figure 8.** TEM images of  $\text{Na}_2\text{SiF}_6$  crystals before (a) and after (b) exposure to electron beam for about 20 s.

larger size and regular structure appear (Figure 7c), while these crystals cannot be observed in the original zeolite and PS/zeolite composite. Combined with the information provided by the XRD, FTIR, and TG analysis, we can draw the conclusion that these crystals are the newly formed crystal  $\text{Na}_2\text{SiF}_6$ . With the extension of HF etching time to 24 h, it can be clearly seen that the  $\text{Na}_2\text{SiF}_6$  crystals transform to a branched structure from the edges while the center parts of these crystals remain as smooth facets (Figure 7d). When the HF etching process further proceeds, microflowers are formed (see Figure 1).

TEM examination was performed on the cracked crystals obtained with a HF etch time of 5 h (Figure 7c). When examining the  $\text{Na}_2\text{SiF}_6$  crystals under TEM, we found that they first appeared as completely dark, as shown in Figure 8a. However, after the crystals were exposed to the electron beam for about 20 s, they presented as a much looser structure with uneven density distribution through the crystals (Figure 8b). We speculate that this may result from the depletion of the polymer on the  $\text{Na}_2\text{SiF}_6$  crystals under the attack of the electron beam irradiation because the polymer on the crystals is much more sensitive to electron beam than the inorganic component.

**Microflowers of Other Polymers.** Using methyl methacrylate (MMA) or divinylbenzene (DVB) as the precursor monomer and via the same procedures as were used to prepare PS microflowers, we also prepared flowerlike structures (Figure 9). This indicates that the present method is a versatile route to prepare polymer of flowerlike structure at suitable conditions. Comparing Figures 1 and 9, it can be seen that the microflowers of different polymers have different morphologies.

**Formation Mechanism of the Microflowers.** Although there are several reports on the synthesis of inorganic materials with

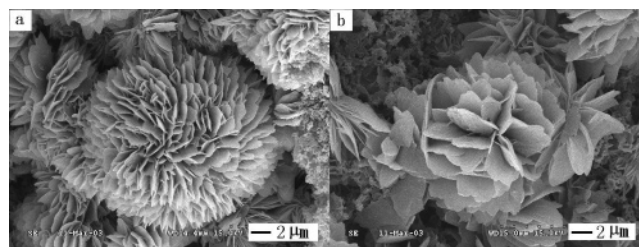


**Figure 9.** Flowerlike structures prepared from composites of zeolite and PMMA (a) and PDVB (b).

flowerlike structures, their formation mechanism cannot be implanted to the present work.<sup>33,35,36</sup> Many reports suggest that macromolecules can bind to nanocrystal surfaces to produce inorganic–organic particles with different shapes and sizes that can act as hybrid building blocks in aggregation-based pathways of crystal growth.<sup>34–36</sup>

On the basis of the above characterization and analysis, here we try to propose a possible mechanism of the formation of the microflowers. With the aid of *sc*  $\text{CO}_2$ , the resulted polymer distributes uniformly in the zeolite, which is supported by the fact that the original zeolite can dissolve in HF aqueous solution within 10 min, while the composite can exist for much longer time at the same condition as discussed above. During the treatment of polymer/zeolite composite with HF aqueous solution, HF and water molecules penetrate into the composite and react with the zeolite to generate species such as  $\text{Na}^+$ ,  $\text{SiF}_6^{2-}$ . However, a relatively long time is needed both for the inorganic species to diffuse into the bulk solution from the composite, and for  $\text{H}^+$  and  $\text{F}^-$  in the bulk solution to diffuse into the composite because the polymer in the composite prevents their faster diffusion. In addition, the solubility of  $\text{Na}_2\text{SiF}_6$  in water is relatively low.<sup>32</sup> Therefore, supersaturation is reached soon, and the  $\text{Na}^+$  and  $\text{SiF}_6^{2-}$  precipitate in the form of  $\text{Na}_2\text{SiF}_6$  crystals. Meanwhile, the confined PS is liberated. The polymer and  $\text{Na}_2\text{SiF}_6$  nearby have a strong tendency to assemble, respectively, to form aggregates with alternate polymeric and inorganic layers during this process, as is also evidenced by Figure 8. The driving force for the assembly of the polymeric and inorganic component, respectively, is the great difference between their physicochemical natures. With the extension of HF treating time, the  $\text{Na}_2\text{SiF}_6$  layers gradually dissolve and diffuse into the bulk solution, and, due to the insoluble nature of the polymer in HF solution, the polymeric layers are retained, and the flower petals are formed by reorganization of the polymer layers as the  $\text{Na}_2\text{SiF}_6$  nearby is dissolved slowly.

Our experiments showed that if the composite was treated at higher temperature (e.g., 50 °C) or with stirring, flowerlike structure could not be obtained. The reason may be that under these conditions,  $\text{Na}^+$ ,  $\text{SiF}_6^{2-}$  produced from the reaction of HF with zeolite can diffuse into the bulk solution with a faster speed. Therefore, supersaturation cannot be reached and the crystallization of  $\text{Na}_2\text{SiF}_6$  cannot occur, or it is dissolved quickly after formation. We also carried out experiments in which styrene was filled in the zeolite host by immersing the host in the liquid monomer and kept the other conditions the same as above, and the microflowers could not be obtained, suggesting that *sc*  $\text{CO}_2$ -aided impregnation of the monomer into the host is important to obtain the well-developed microflowers because *sc*  $\text{CO}_2$  can disperse the precursor throughout the zeolite uniformly due to its high diffusivity and near zero surface tension. These experiments support the possible mechanism discussed above.

## Conclusions

Unique microscale flowerlike polymer superstructures with uniform petals in nanoscale have been fabricated using zeolite as the porous host. In this method, a polymer/zeolite composite is first prepared with the aid of SC CO<sub>2</sub>. Subsequent HF solution treatment of the composites results in self-assembling of the polymer and inorganic components to form alternate polymeric and inorganic layers. Further HF treatment removes the inorganic layers and leaves the polymer layers in a flowerlike structure.

## References and Notes

- (1) Wu, C. G.; Bein, T. *Science* **1994**, *264*, 1757.
- (2) Lee, K.; Kim, J.; Cheon, M. J. *Adv. Mater.* **2001**, *13*, 517.
- (3) Sakamoto, Y.; Fukuoka, A.; Higuchi, T.; Shimomura, N.; Inagaki, S.; Ichikawa, M. *J. Phys. Chem. B* **2004**, *108*, 853.
- (4) Zhang, Z. T.; Pan, Z. W.; Mahurin, S. M.; Dai, S. *Chem. Commun.* **2003**, 2584.
- (5) Liam, M. W.; Peter, P. E.; Paul, A. A. *Chem. Commun.* **2002**, 2894.
- (6) Stuky, G. D.; MacDongall, J. E. *Science* **1990**, *247*, 669.
- (7) Parala, H.; Winkler, H.; Kolbe, M.; Wohlfart, A.; Fischer, R. A.; Schmechel, R.; von Seggern, H. *Adv. Mater.* **2000**, *12*, 1050.
- (8) Wang, S.; Choi, D. G.; Yang, S. M. *Adv. Mater.* **2002**, *14*, 1311.
- (9) Kageyama, K.; Tamazawa, J.; Aida, T. *Science* **1999**, *285*, 2113.
- (10) Jang, J.; Lim, B.; Lee, J.; Hyeon, T. *Chem. Commun.* **2001**, 83.
- (11) Johnson, S. A.; Brigham, E. S.; Ollivier, P. J.; Mallouk, T. E. *Chem. Mater.* **1997**, *9*, 2448.
- (12) Ma, Z.; Kyotani, T.; Liu, Z.; Terasaki, O.; Tomita, A. *Chem. Mater.* **2001**, *13*, 4413.
- (13) Ryoo, R.; Joo, S. H.; Jun, S. J. *J. Phys. Chem. B* **1999**, *103*, 7743.
- (14) Kim, S. W.; Son, S. U.; Lee, S. I.; Hyeon, T.; Chung, Y. K. *J. Am. Chem. Soc.* **2000**, *122*, 1550.
- (15) Domingo, C.; García-Carmona, J.; Llibre, J.; Rodríguez-Clemente, R. *Adv. Mater.* **1998**, *10*, 672.
- (16) Coleman, N. R. B.; Ryan, K. M.; Spalding, T. R.; Holmes, J. D.; Morris, M. A. *Chem. Phys. Lett.* **2001**, *343*, 1.
- (17) Coleman, N. R. B.; Morris, M. A.; Spalding, T. R.; Holmes, J. D. *J. Am. Chem. Soc.* **2001**, *123*, 187.
- (18) Coleman, N. R. B.; O'Sullivan, N.; Ryan, K. M.; Crowley, T. A.; Morris, M. A.; Spalding, T. R.; Steytler, D. C.; Holmes, J. D. *J. Am. Chem. Soc.* **2001**, *123*, 7010.
- (19) Crowley, T. A.; Ziegler, K. J.; Lyons, D. M.; Erts, D.; Olin, H.; Morris, M. A.; Holmes, J. D. *Chem. Mater.* **2003**, *15*, 3518.
- (20) McHugh, M. A. V.; Krukoni, J. *Supercritical Fluid Extraction: Principle and Practice*, 2nd ed.; Butterworth-Heinemann: Boston, 1994.
- (21) Fu, Y.; Palo, D. R.; Erkey, C.; Weiss, R. A. *Macromolecules* **1997**, *30*, 7611.
- (22) Cooper, A. I. *J. Mater. Chem.* **2000**, *10*, 207.
- (23) Kazarian, S. G. *Polym. Sci., Ser. C* **2000**, *42*, 78.
- (24) Liu, Z.; Dai, X.; Xu, J.; Han, B.; Zhang, J.; Wang, Y.; Huang, Y.; Yang, G. *Carbon* **2004**, *42*, 458.
- (25) Watkins, J. J.; McCarthy, T. J. *Macromolecules* **1994**, *27*, 4845.
- (26) Li, D.; Han, B. X. *Macromolecules* **2000**, *33*, 4550.
- (27) Arora, K. A.; Lesser, A. J.; McCarthy, T. J. *Macromolecules* **1997**, *32*, 22562.
- (28) Liu, Z.; Dong, Z.; Han, B.; Wang, J.; He, J.; Yang, G. *Chem. Mater.* **2002**, *14*, 4619.
- (29) Moller, K.; Bein, T. R.; Fischer, X. *Chem. Mater.* **1998**, *10*, 1841.
- (30) Breck, D. W. *Zeolite Molecular Sieves*; John-Wiley: New York, 1974.
- (31) Song, S.; Lopez-valdivieso, A.; Lu, S.; Ouyang, J. *Powder Technol.* **2002**, *123*, 178.
- (32) Simons, J. H. *Fluoride Chemistry*; Academic Press: New York, 1950; Vol. 1.
- (33) Zhang, J.; Sun, L. D.; Yin, J. L.; Su, H. L.; Liao, C. S.; Yan, C. H. *Chem. Mater.* **2002**, *14*, 4172.
- (34) Yu, S. H.; Colfen, H.; Antonietti, M. *Chem.-Eur. J.* **2002**, *8*, 2937.
- (35) Colfen, H.; Mann, S. *Angew. Chem., Int. Ed.* **2003**, *42*, 2350.
- (36) Colfen, H.; Qi, L.; Mastai, Y.; Borger, L. *Cryst. Growth Des.* **2002**, *2*, 191.